A Tau-Targeted Multifunctional Nanocomposite for Combinational Therapy of Alzheimer's Disease

Qing Chen,[‡,#] Yang Du,[†,#] Kai Zhang,[‡,#] Zeyu Liang,[†,#] Jinquan Li,[†] Hao Yu,[†] Rong Ren,[§] Jin Feng,[‡] Zhiming Jin,[o] Fangyuan Li,[†,∥] Jihong Sun,[⊥] Min Zhou,[‡] Qinggang He,[§] Xiaolian Sun,[Ψ] Hong Zhang,[‡,◊] Mei Tian,[‡,◊,*] Daishun Ling[†,∥,*]

[‡]Department of Nuclear Medicine and PET/CT Center, The Second Affiliated Hospital, School of Medicine, Zhejiang University, Hangzhou, Zhejiang 310009, P.R. China,

[†]Institute of Pharmaceutics, College of Pharmaceutical Sciences, Zhejiang University, 866 Yuhangtang Road, Hangzhou, Zhejiang 310058, P. R. China,

[∥] Key Laboratory of Biomedical Engineering of the Ministry of Education, College of Biomedical Engineering & Instrument Science, Zhejiang University, Hangzhou, Zhejiang 310058, P.R. China,

[◊]Collaborative Innovation Center for Brain Science, Fudan University, Shanghai 200032, P. R. China,

[§]College of Chemical & Biological Engineering, Zhejiang University, Hangzhou, Zhejiang 310027, P. R. China,

[⊥]Department of Radiology, Sir Run Run Shaw Hospital, Zhejiang University School of Medicine, Hangzhou, Zhejiang 310016, P. R. China,

[Ψ] Department of Pharmaceutical Analysis, China Pharmaceutical University, Nanjing 210009, P. R. China,

[o] Jiangsu Huayi Technology Limited Company, Changshu, Jiangsu 215522, P. R. China.
[#] These authors contributed equally to this work.

Corresponding Authors

Daishun Ling: lingds@zju.edu.cn; Mei Tian: Meitian@zju.edu.cn

Supporting figures

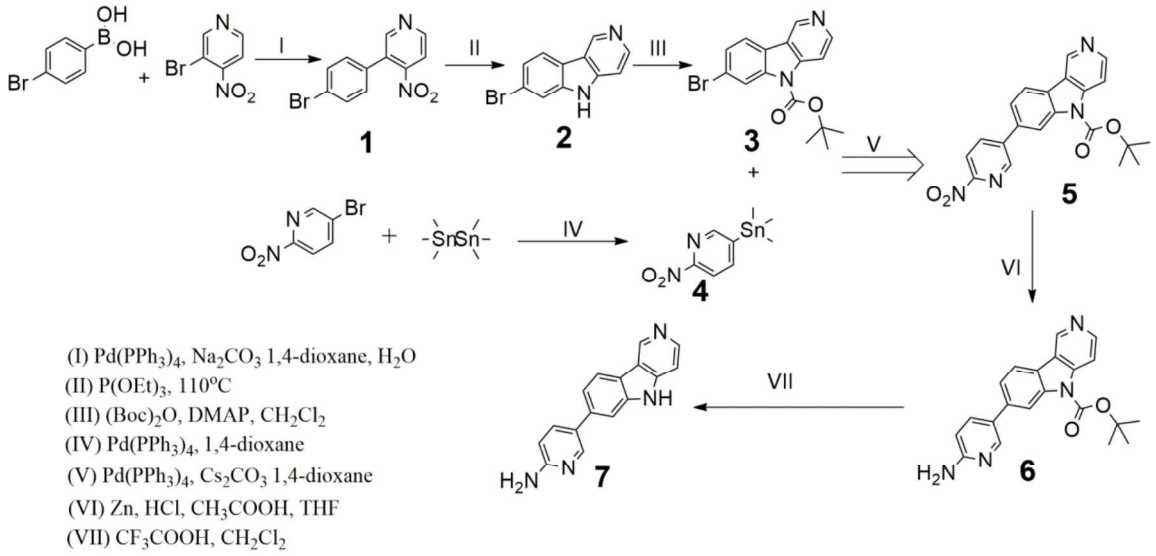

Figure S1. Synthetic scheme of amino-T807.

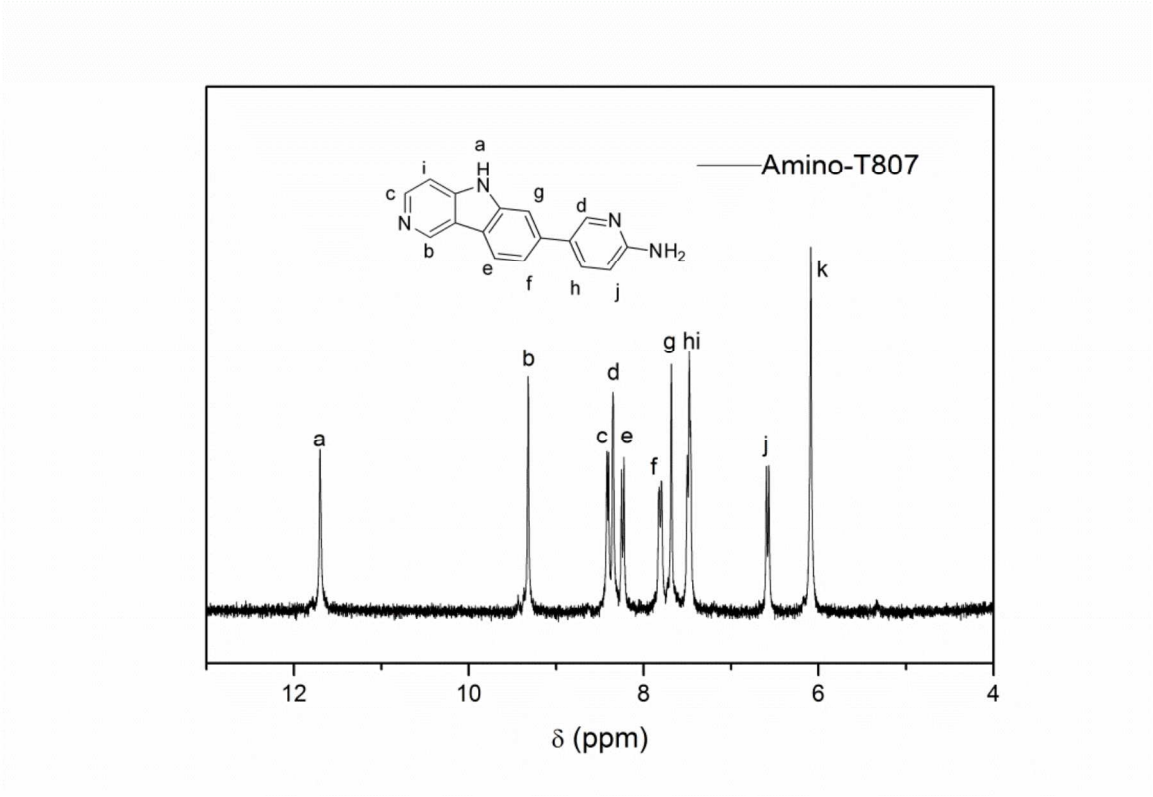

Figure S2. ^{1}H-NMR analysis of amino-T807.

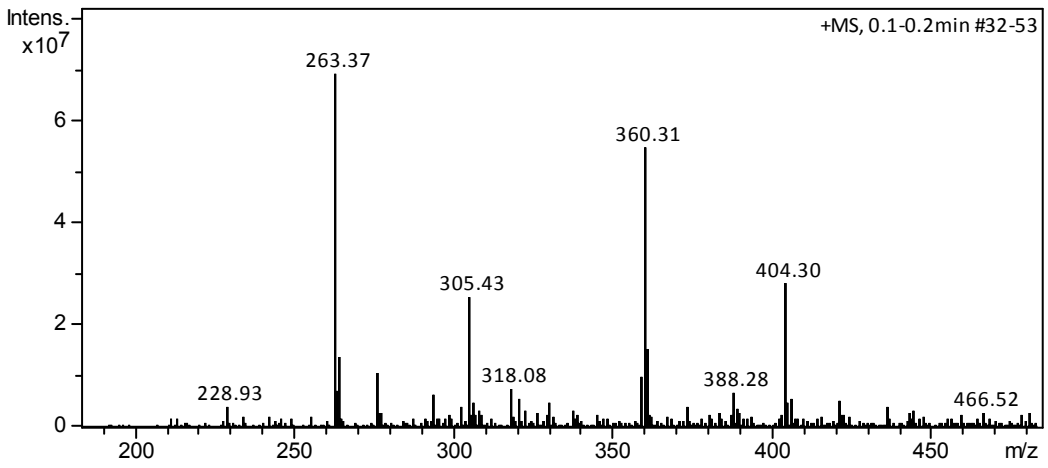

Figure S3. Mass spectrum of amino-T807.

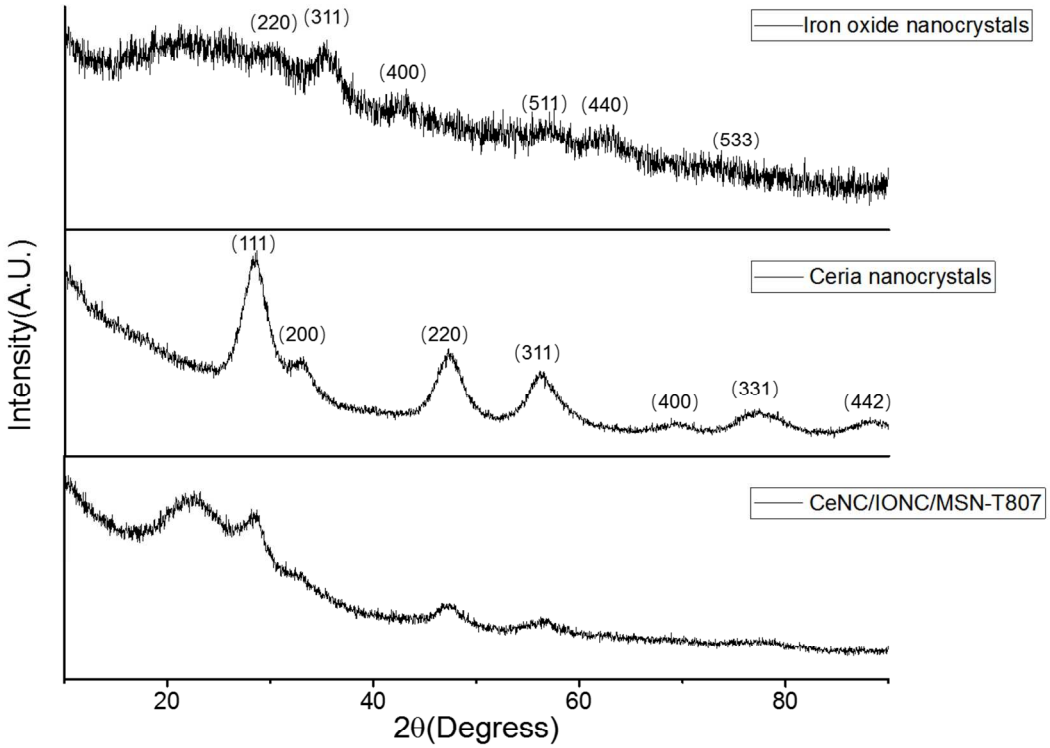

Figure S4. X-Ray Diffraction (XRD) pattern of iron oxide nanocrystals, ceria nanocrystals and CeNC/IONC/MSN-T807.

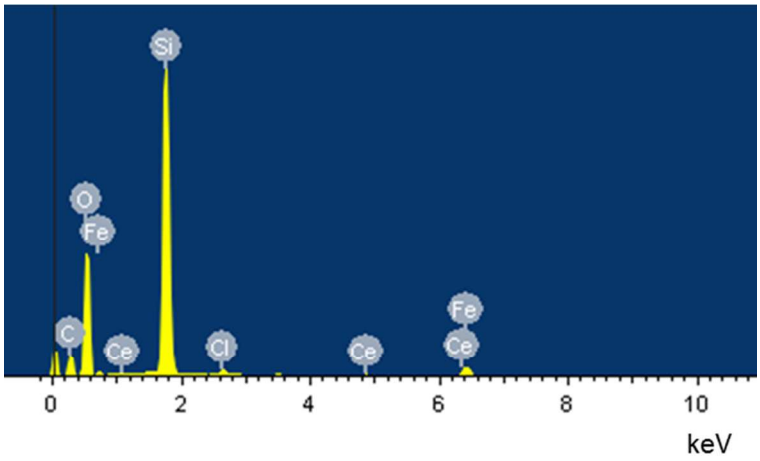

Element	weight (%)	Atoms (%)
C K	23.58	33.23
O K	48.29	51.08
Si K	23.93	14.42
Cl K	0.59	0.28
Fe K	3.00	0.91
Ce L	0.60	0.07
Total	100.00	

Figure S5. Energy-dispersive X-ray spectroscopy of CeNC/IONC/MSN-T807 (left) and quantification of different elements (right).

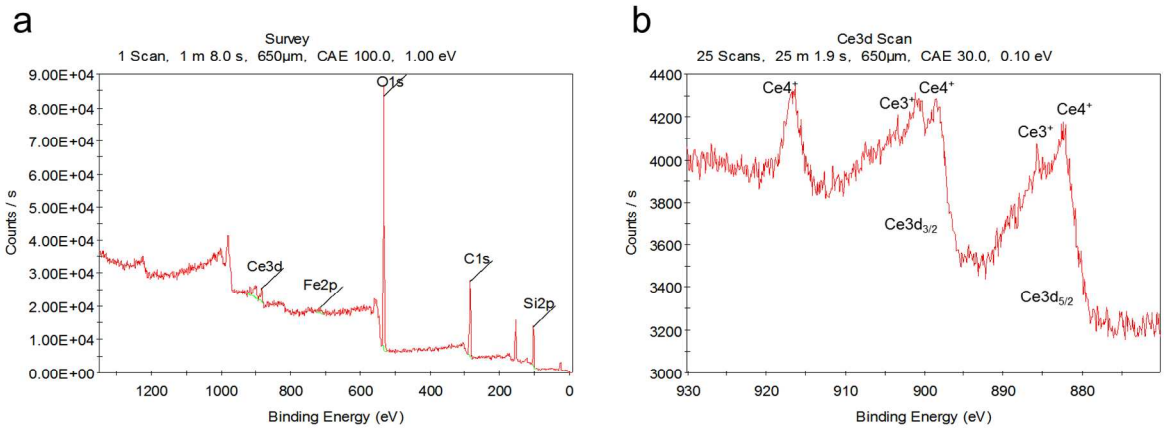

Figure S6. X-ray photoelectron spectroscopy (XPS) analysis of CeNC/IONC/MSN-T807. (a) XPS analysis from 0 to 1300 eV, (b) amplification section from 870 to 930 eV.

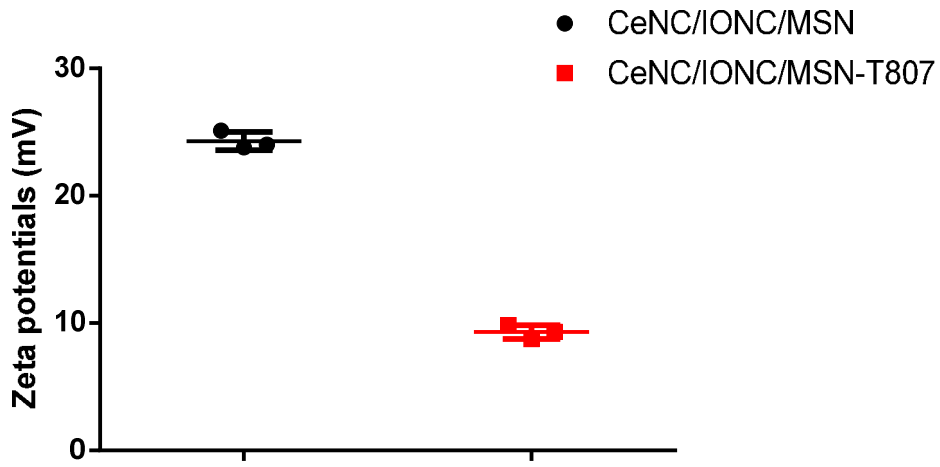

Figure S7. Zeta potentials of CeNC/IONC/MSN and CeNC/IONC/MSN-T807.

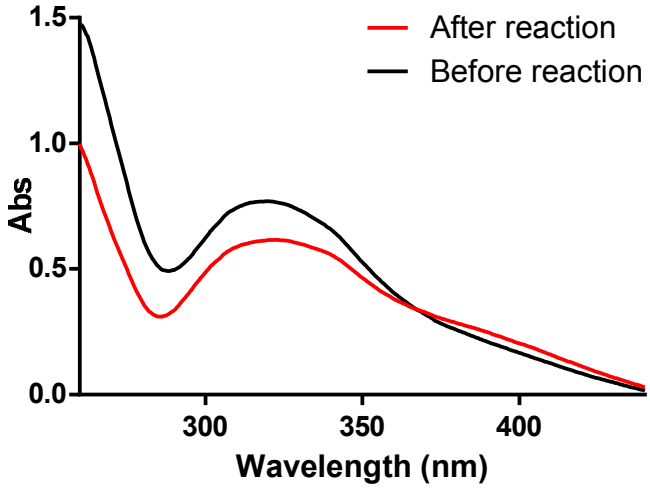

Figure S8. The UV absorption spectrum of the supernatant before and after reaction.

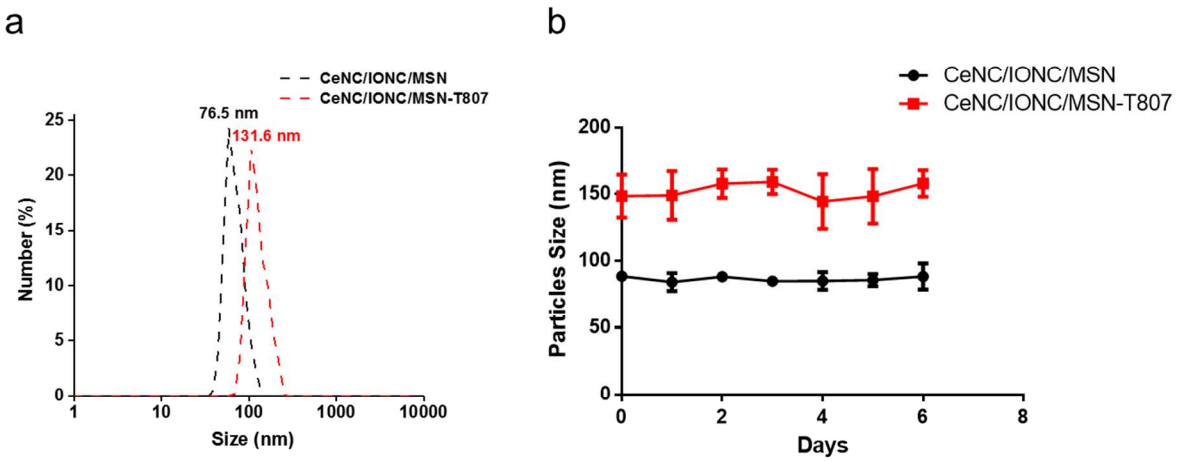

Figure S9. (a) Hydrodynamic diameters measured by DLS of CeNC/IONC/MSN and CeNC/IONC/MSN-T807 in water and (b) The change of average particle size for one week storage.

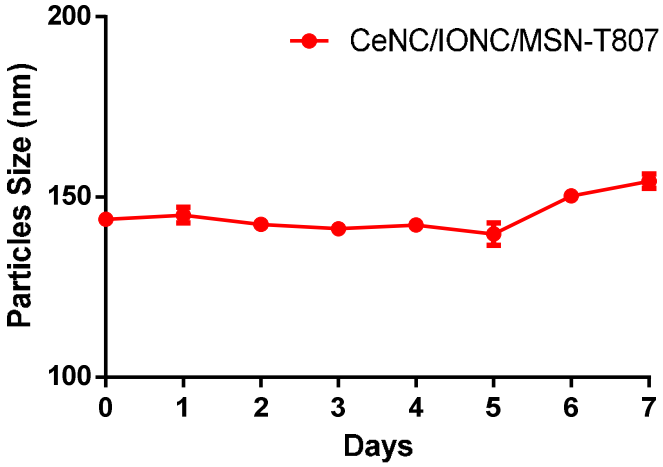

Figure S10. The change of average particle size of CeNC/IONC/MSN-T807 in cell culture medium (DMEM + 10 % FBS).

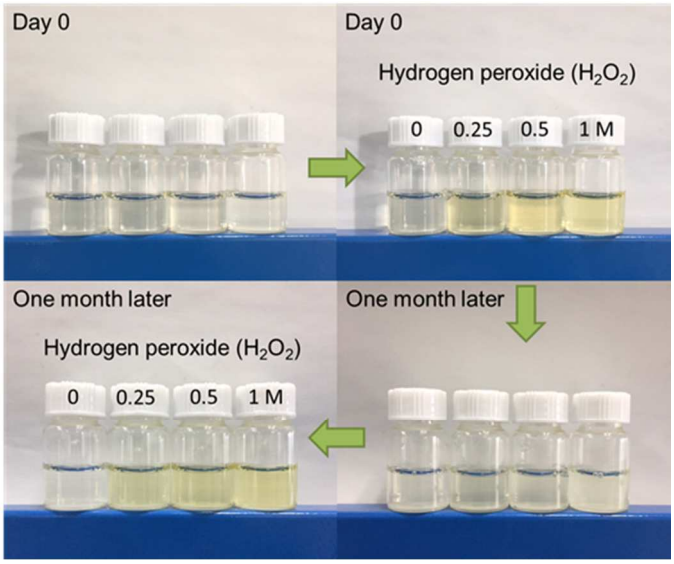

Figure S11. Autocatalytic behavior of CeNC/IONC/MSN-T807. Photographs of the aqueous solution of CeNC/IONC/MSN-T807 in the absence and presence of H_2O_2 exhibiting reversible color changes.

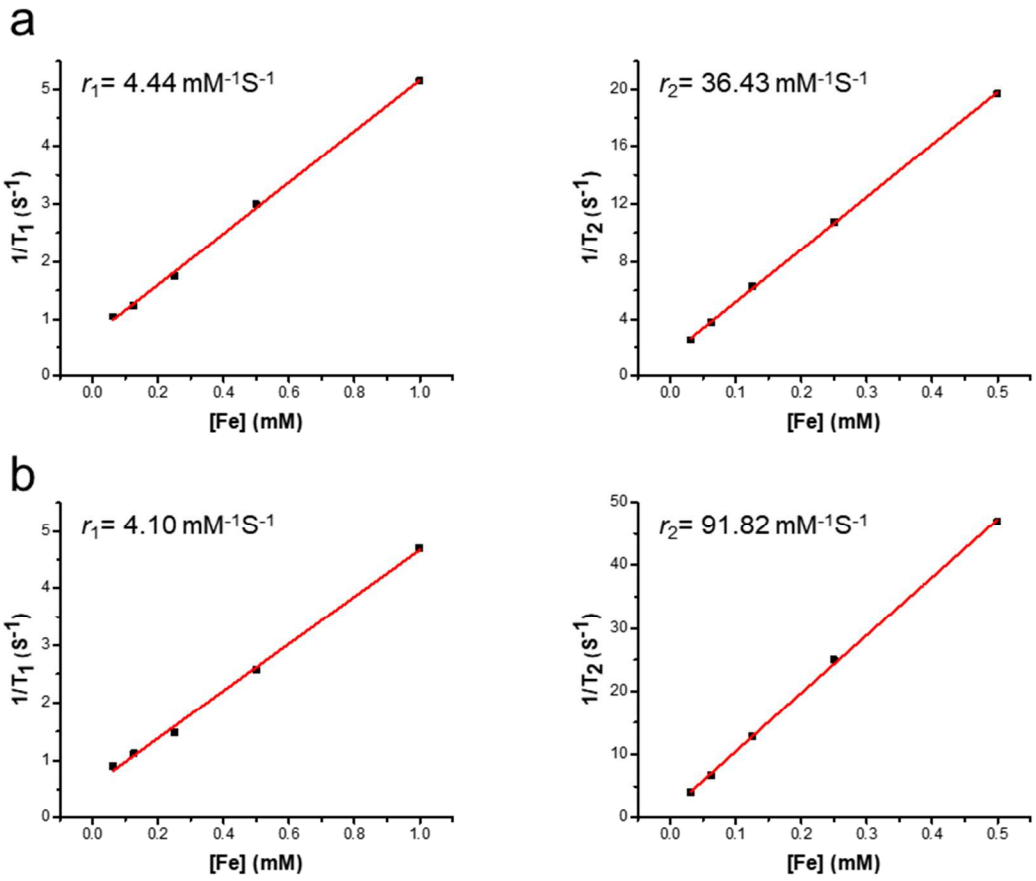

Figure

Figure S12. (a) Plot of $1/T_1$ and $1/T_2$ over Fe ions concentration of IONCs, the slope indicates the specific relaxivity r_1 and r_2. (b) Plot of $1/T_1$ and $1/T_2$ over Fe ions concentration of CeNC/IONC/MSN, the slope indicates the specific relaxivity r_1 and r_2.

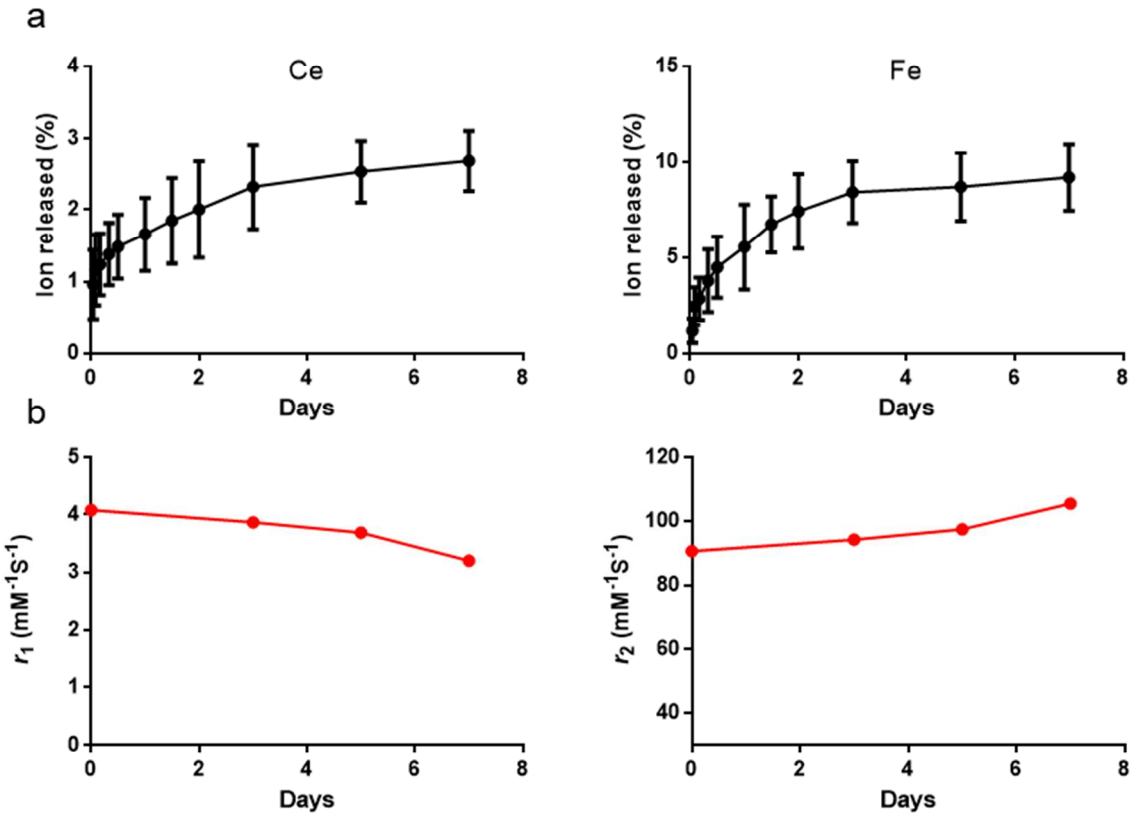

Figure S13. (a) The cerium and iron ions release of CeNC/IONC/MSN-T807 in the cell culture medium (DEME + 10% FBS) during incubation. Error bars represent standard deviation (n = 3 per group). (b) The relaxivity change of CeNC/IONC/MSN-T807 in the cell culture medium (DEME + 10% FBS) during incubation.

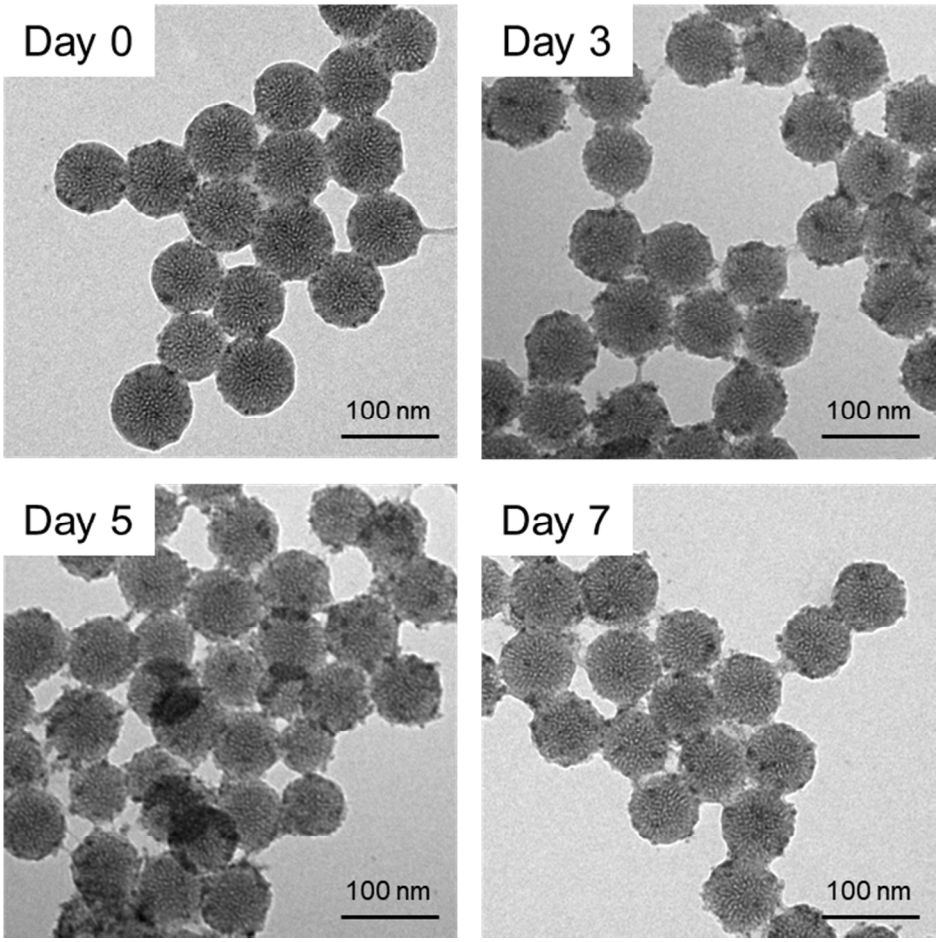

Figure S14. TEM images of CeNC/IONC/MSN-T807 in cell culture medium (DEME + 10% FBS) at the indicated times.

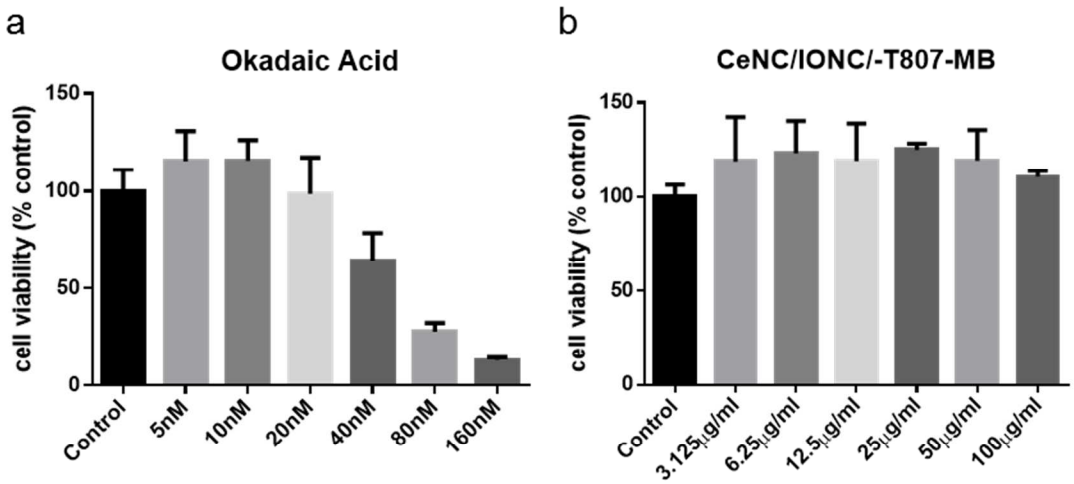

Figure S15. (a) Cell viability measured by CCK8 assay of SH-SY5Y cells treated with different concentrations of OA for 12 h, (b) Cell viability of different concentrations of CeNC/IONC/MSN-T807-MB in SH-SY5Y cells after 12 h of exposure.

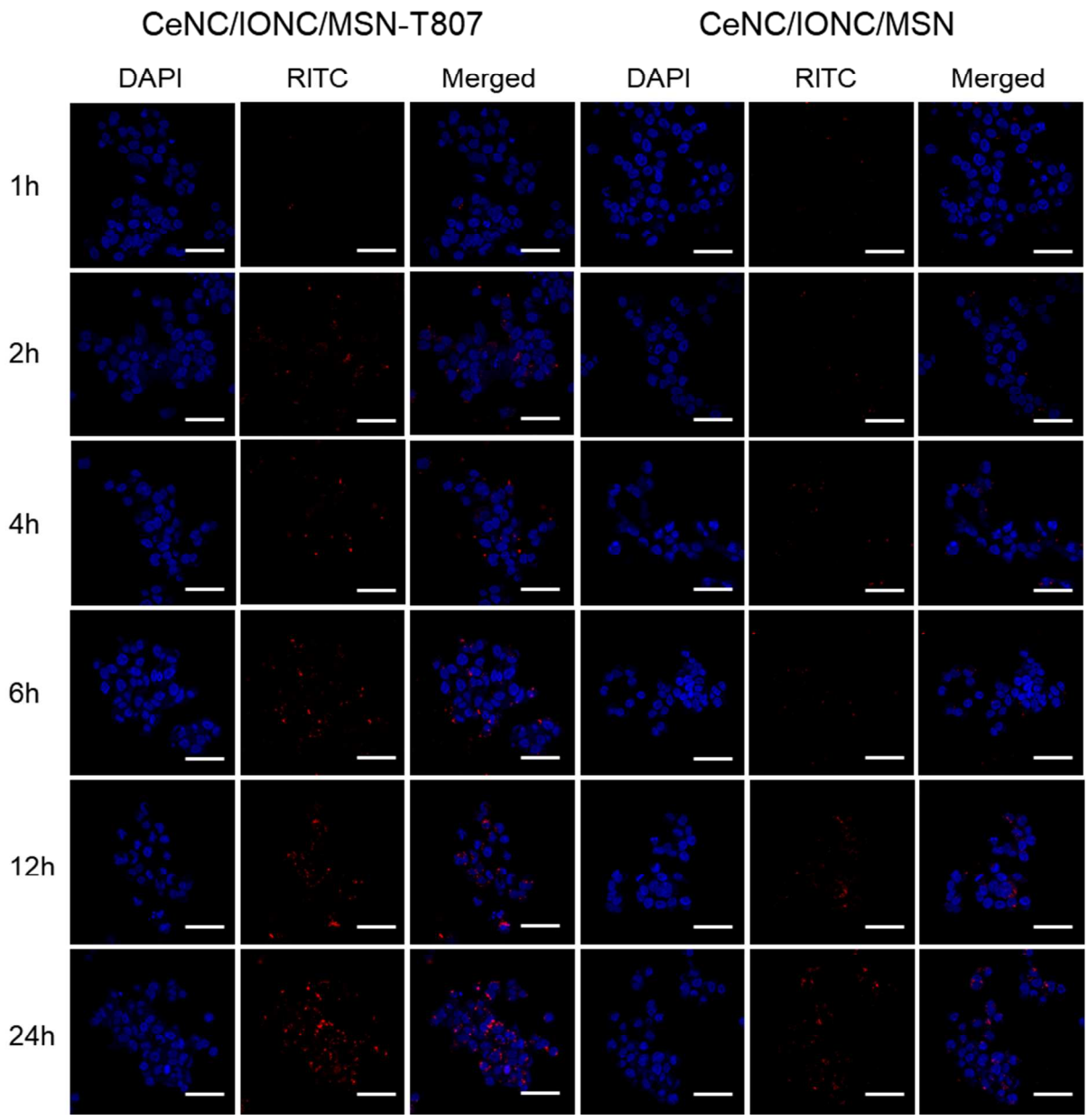

Figure S16. Confocal fluorescence images of OA treated SH-SY5Y cells treated with CeNC/IONC/MSN-T807 or CeNC/IONC/MSN at a serial time points. Cells were stained with DAPI (blue). CeNC/IONC/MSN-T807 and CeNC/IONC/MSN were labeled with RITC (red) (Scale bar = 50 μm).

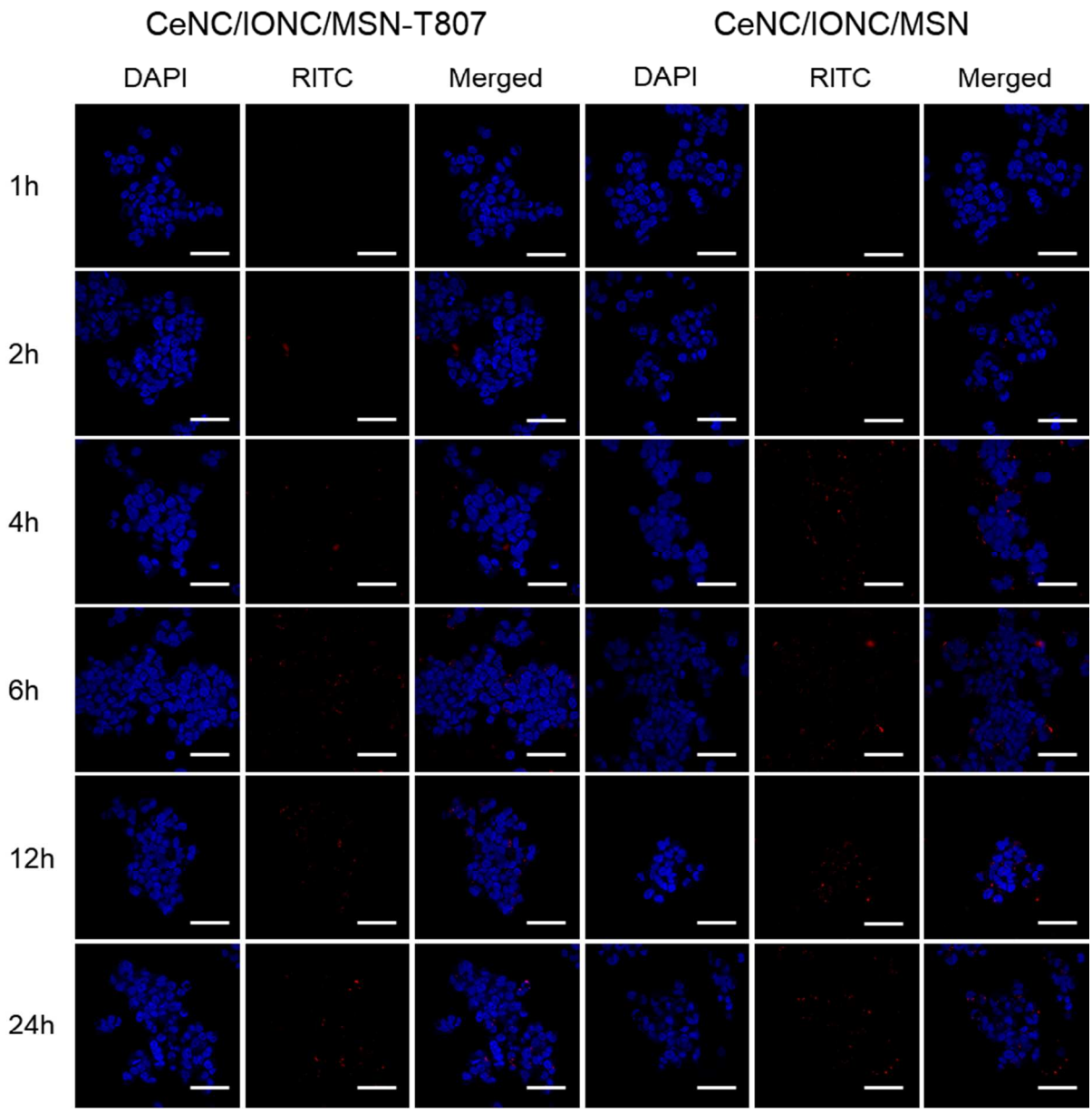

Figure S17. Confocal fluorescence images of SH-SY5Y cells treated with CeNC/IONC/MSN-T807 or CeNC/IONC/MSN at a serial time points. Cells were stained with DAPI (blue). CeNC/IONC/MSN-T807 and CeNC/IONC/MSN were labeled with RITC (red) (Scale bar = 50 μm).

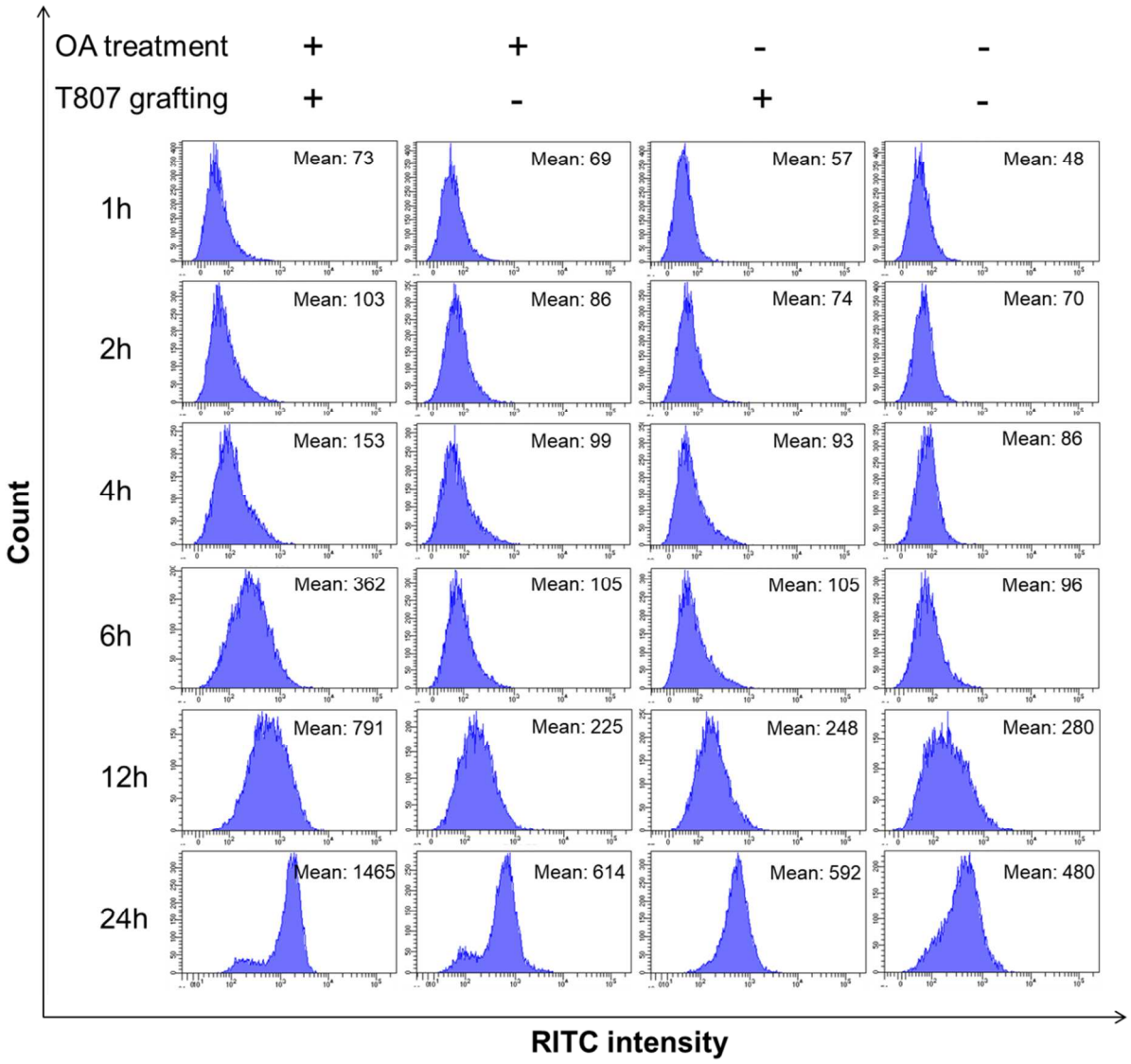

Figure S18. Flow cytometry analysis of the internalization of CeNC/IONC/MSN-T807 or CeNC/IONC/MSN in SH-SY5Y cells with or without OA treatment at the indicated incubation times.

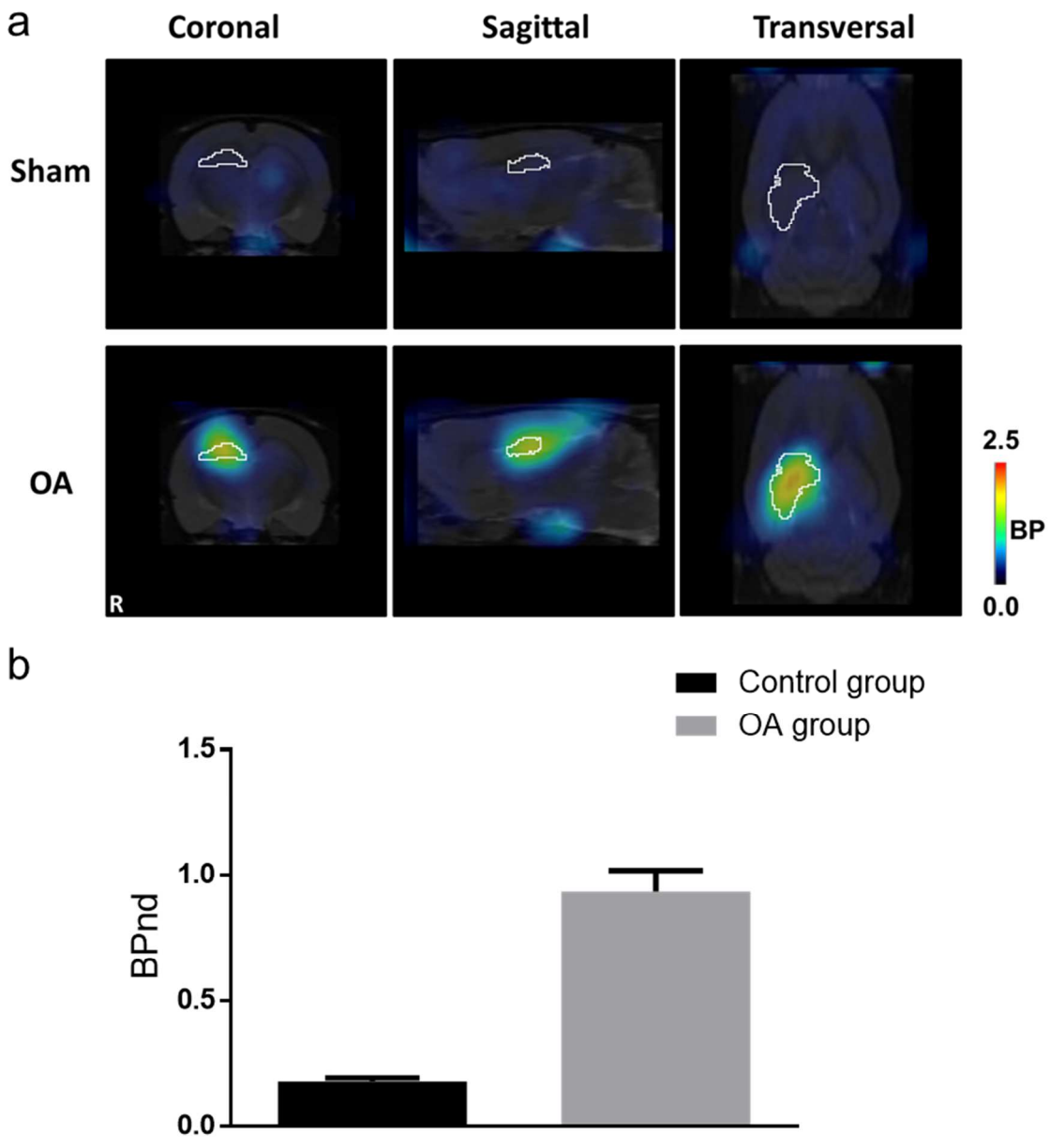

Figure S19. Verification of the established AD model rats. (a) PET/CT images of Sham group (upper) and OA group (lower). (b) BPnd values of indicated groups (n=8 per group).

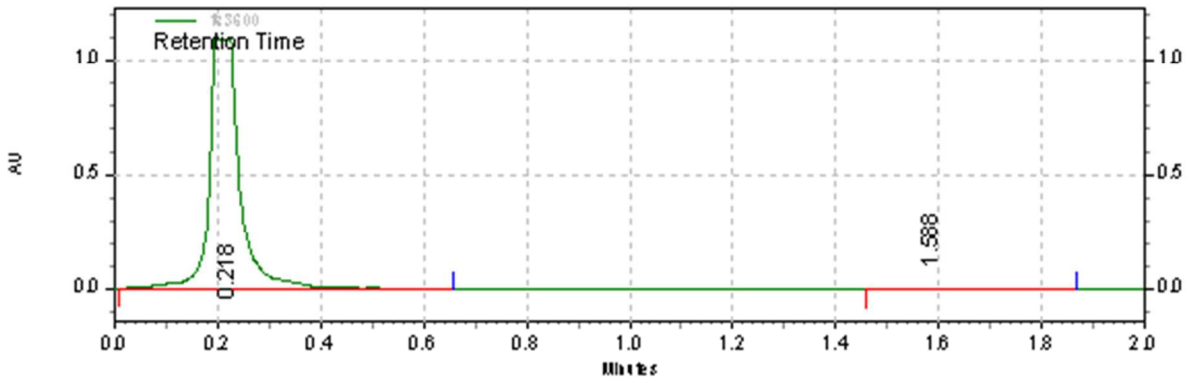

Results

Time	Area	Area %	Height	Height %
0.218	4559985	99.57	1088261	99.77

Figure S20. The radiolabeling efficiency of CeNC/IONC/MSN-T807.

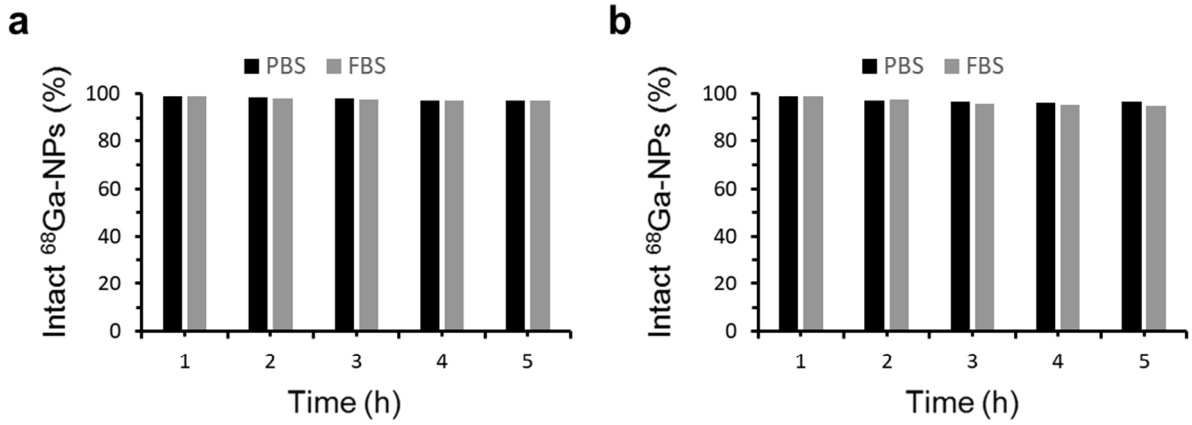

Figure S21. Stability of radiolabeled CeNC/IONC/MSN-T807 (a) and CeNC/IONC/MSN (b) in PBS or FBS.

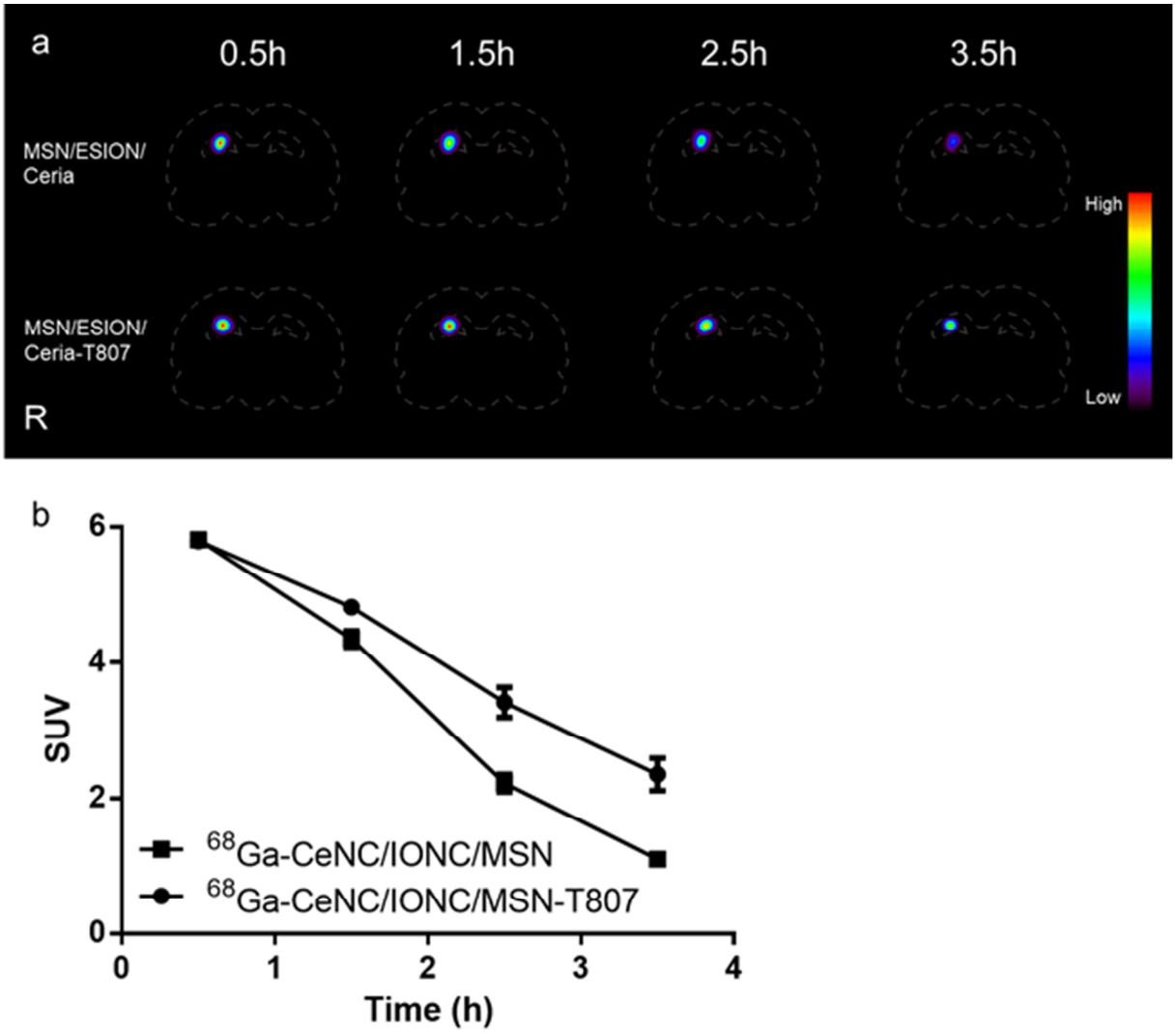

Figure S22. (a) *In vivo* PET images of AD model rat brain after administration of ^{68}Ga-CeNC/IONC/MSN (upper) and ^{68}Ga-CeNC/IONC/MSN-T807 (lower) at each indicated time points. (b) SUV values of ^{68}Ga-CeNC/IONC/MSN and ^{68}Ga-CeNC/IONC/MSN-T807 groups at corresponding time points. Error bars represent standard deviation (n = 3 per group).

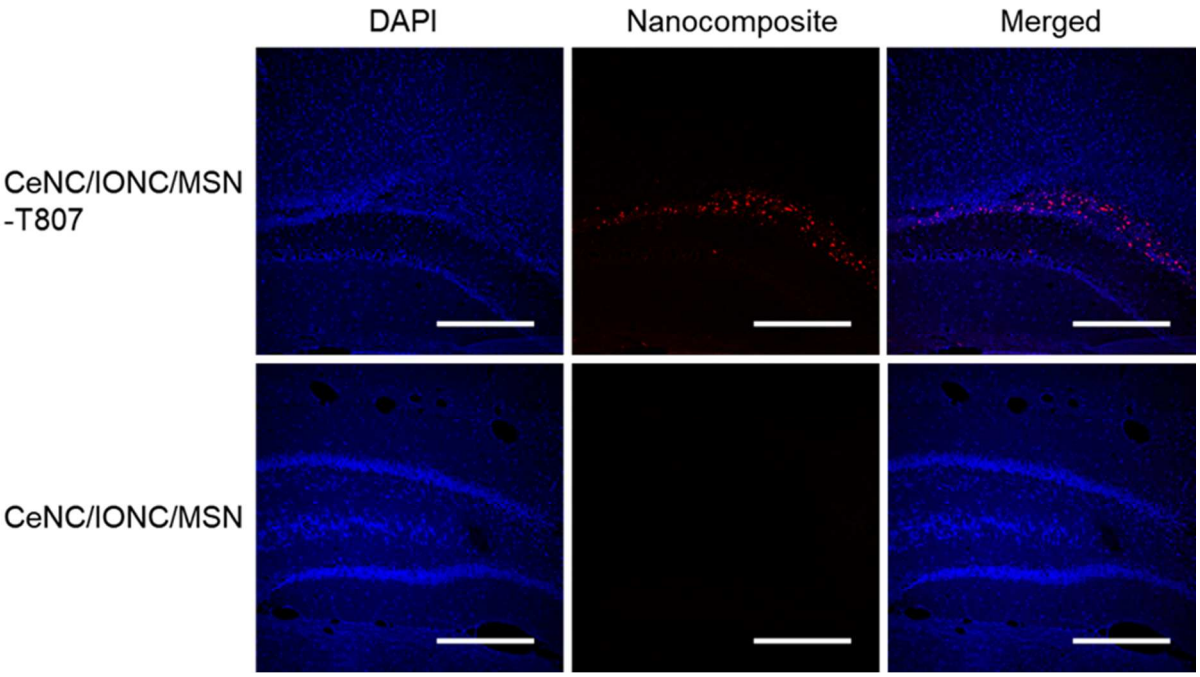

Figure S23. Confocal fluorescence images of RITC (red) labeled CeNC/IONC/MSN-T807 and CeNC/IONC/MSN in the brain slices of AD model rats at 6h after injection. Cells were stained with DAPI (blue) (Scale bar = 400 μm).

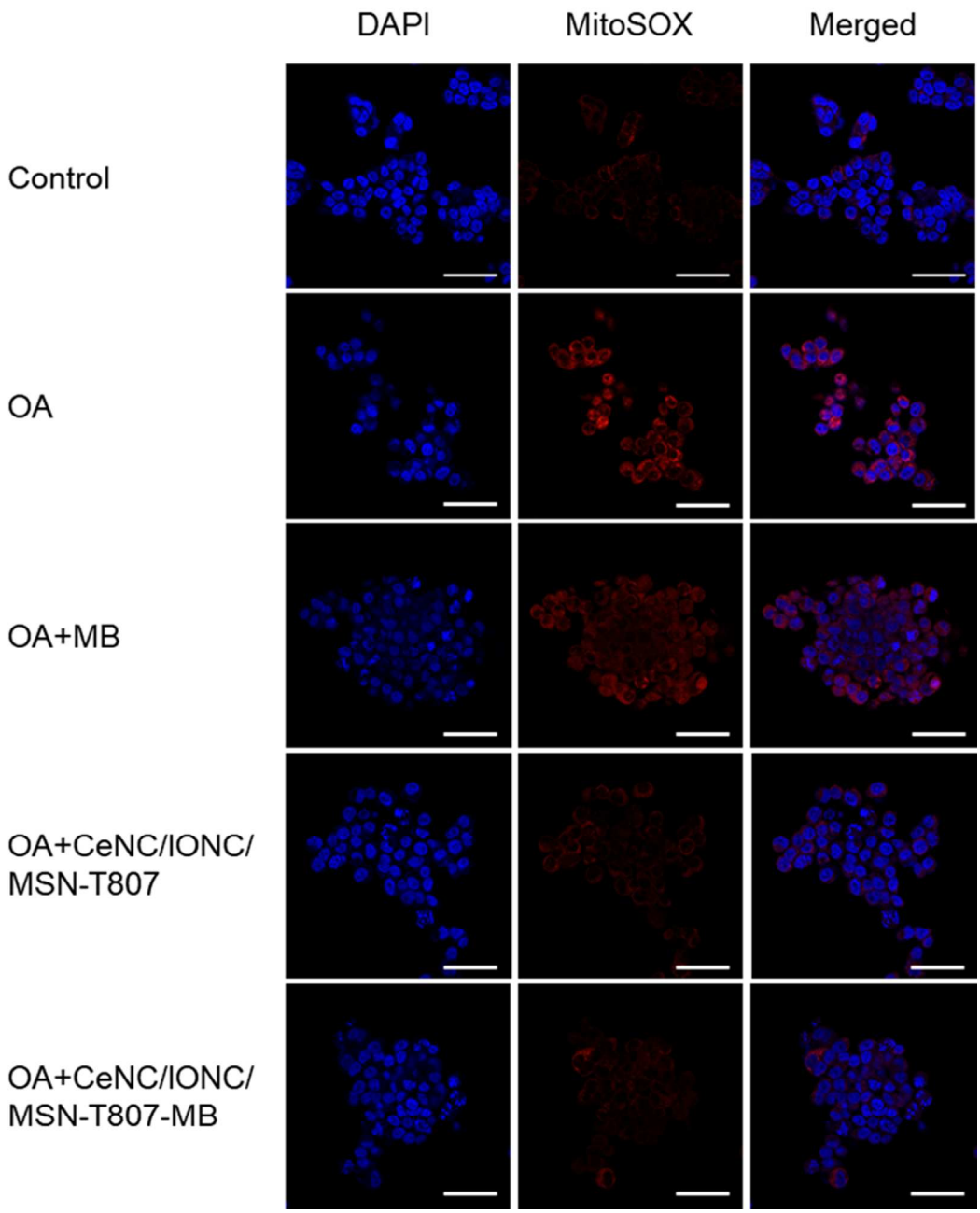

Figure S24. The confocal images of mitochondrial ROS accumulation in SH-SY5Y cells. Cells were stained with DAPI (blue), MitoSOX (Red) (Scale bar = 50 μm).

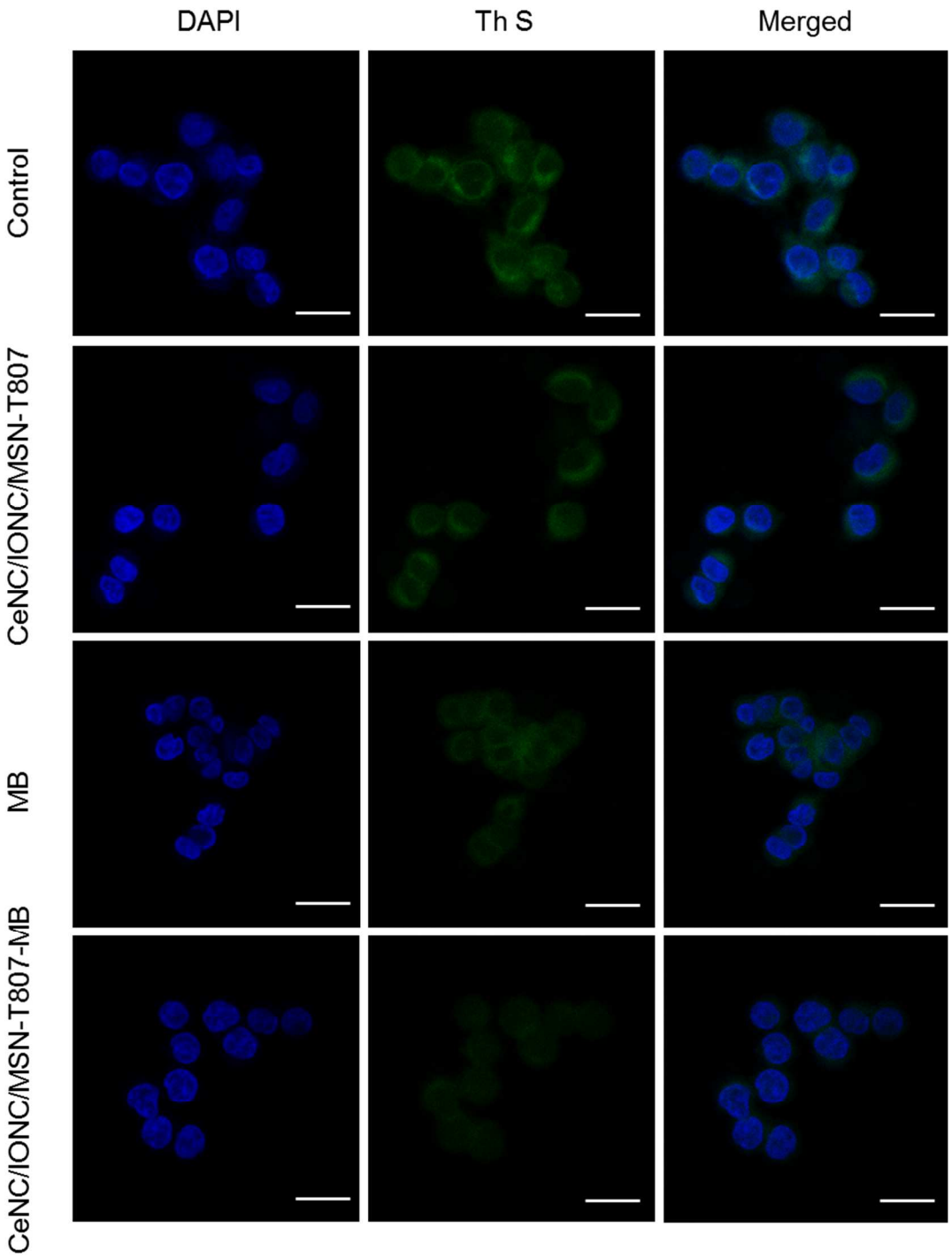

Figure S25. Inhibition of tau aggregation in cells. Confocal fluorescence images of OA treated SH-SY5Y cells co-incubated with CeNC/IONC/MSN-T807, CeNC/IONC/MSN-T807-MB or MB. Cells were stained with DAPI (blue) and ThS (green). The fluorescence intensity of ThS indicates the degree of tau aggregation (Scale bar = 20 μm).

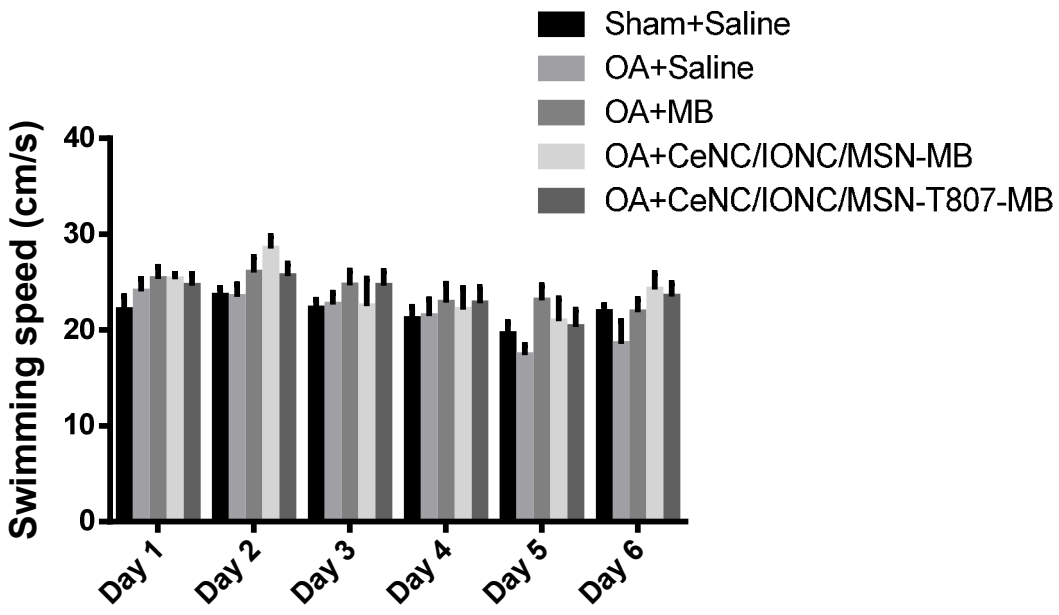

Figure S26. Swimming speed of rats in the hidden platform learning trials and probe trial.

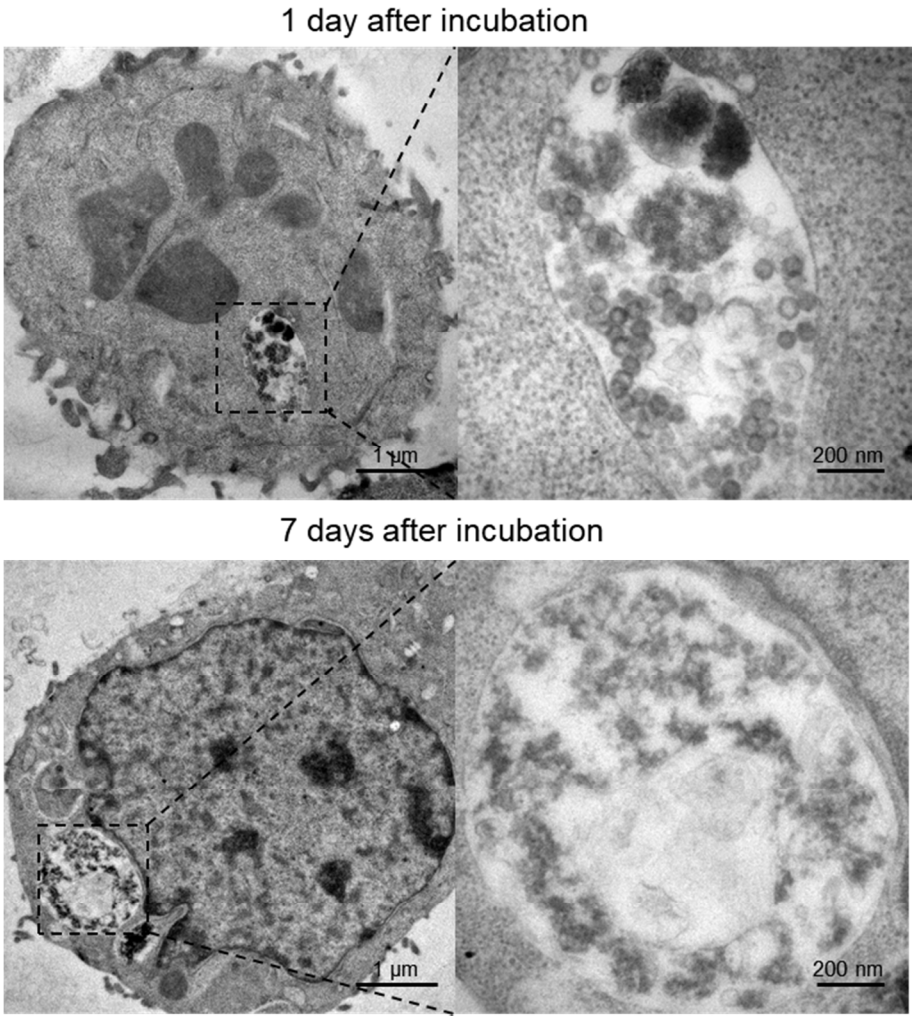

Figure S27. TEM images of CeNC/IONC/MSN-T807-MB in the SH-SY5Y cells at the indicated incubation times.

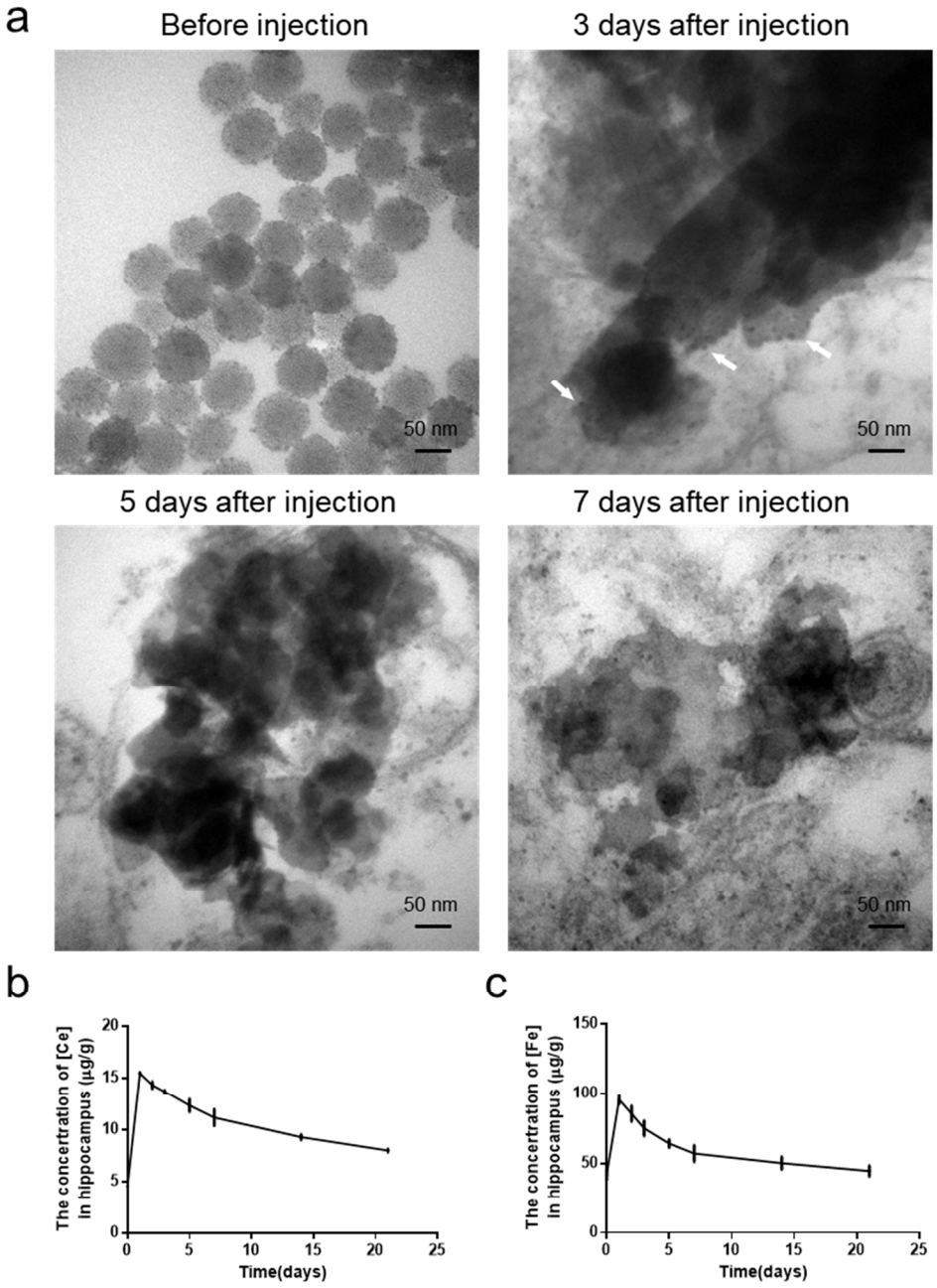

Figure S28. Degradation of CeNC/IONC/MSN-T807-MB in the hippocampal tissue of AD model rats. (a) TEM images of CeNC/IONC/MSN-T807-MB in the hippocampal tissue of AD model rats at the indicated times. White arrows indicate the small nanocrystals on the nanocomposites. (b) The change of the cerium ion concentration in the hippocampal tissue was measured by ICP-MS. (c) The change of the iron ion concentration in the hippocampal tissue was measured by ICP-MS. Error bars represent standard deviation (n = 3 per group).

Table S1. Real-Time PCR Primers and Conditions

Gene	Genbank Accession	Primer Sequences(5'to3')	Size(bp)	Annealing (℃)
Human GAPDH	NM_002046.5	CCATGACAACTTTGGTATCGTGGAA GGCCATCACGCCACAGTTTC	107	60
Human AKT1	NM_005163.2	GCCCCACTTCCCCCAGTTCT CCGCCTCTCCATCCCTCCAA	94	60
Human GSK3	NM_002093.3	GGGACCCAAATGTCAAACTACCA CGAGCATGAGGAGGAATAAGGAT	118	60
Human Bax	NM_004324	CCCTTTTGCTTCAGGGTTTCATCCA CTTGAGACACTCGCTCAGCTTCTTG CACATGACCCCACCGAACTCAAAG A	122	60
Human Caspase3	NM_032991	GACAGACAGTGGTGTTGATGATGA C GCATGGCACAAAGCGACTGGAT	148	60